

## EFFECTS OF STRESS RATIOS ON THE FATIGUE STRENGTHS OF CRUCIFORM FILLET WELDED JOINTS

*By Hirosuke SHIMOKAWA\*, Koei TAKENA\*\*, Fumio ITO\*\*\* and Chitoshi MIKI\*\*\*\**

The fatigue strength of transverse-fillet-welds in the attachment of diaphragms is a decisive factor in the design of box-section truss members. The fatigue strength of this joint is influenced by the profile of the fillet-welds at the scallop and the residual stress created by the corner weld. In order to study the fatigue strength at the ends of the scallops, a real size cruciform model was fabricated, where a pair of rib plates were welded on both sides of a base plate containing four longitudinal weld-beads. The size of the base plate was 45 mm thick and 300 mm wide. Fatigue tests were performed with an electro-hydraulic fatigue testing machine of a dynamic capacity of 4 MN. The tests were performed with stress ratios at 0, -1, -2 and -5.

### 1. INTRODUCTION

The fatigue strength of steel structural members is considered to be influenced by the mean stress, hence in fatigue designs of steel railway bridges<sup>1)</sup> and also the Honshu-Shikoku bridges in Japan<sup>2)</sup>, the influence of the mean stress had been calculated using a parameter  $k(=\sigma_{\min}/\sigma_{\max})$ . However, recent research results have indicated that in fatigue strength of large welded structural members, the mean stress has little effect on the fatigue strengths<sup>3), 4)</sup>. In the design standards for bridges in the United States<sup>5)</sup> and Britain<sup>6)</sup>, the method of fatigue appraisal for welded joints has recently been changed to be checked by the cyclic stress range. In truss members of cable-stayed bridges, such as the Hitsuishijima Bridge and Iwakurojima Bridge (both bridges, main span of 420 m, four railway trucks on the lower deck and four highway lanes on the upper deck), in many cases compressive stresses are larger than tensile stresses (Fig.1). Even though the whole nominal stress is compressive, occasionally fatigue cracks develop in the welded members because such a structure has high residual tensile stresses. For example, in the compression-to-compression cyclic loading tests using longitudinal bead-welded joints, relatively large fatigue cracks developed<sup>2), 7)</sup>. When box section welded girders were tested in completely pulsating bending, there was no difference in the number of fatigue cracks between upper and lower flanges<sup>8)</sup>.

After the development of a crack, the profile of the residual stress changes and the maximum residual stress decreases gradually, thus resulting in the slowing down of the growth of the rate of fatigue cracks. The load-bearing capacities of members against compressive forces do not decrease even when cracks exist; in addition, it is possible to detect these cracks during service inspections. Therefore, it may be overly conservative to use the same allowable stress ranges as in the design of the members where tensile forces are predominant. The present

\* Member of JSCE, Honshu-Shikoku Bridge Authority (Mori Bld. No.22, Toranomon, Minato-ku, Tokyo)

\*\* Member of JSCE, Japan Construction Method and Machinery Research Institute (Oobuchi, Fuji-City, Shizuoka)

\*\*\* Member of JSCE, Dr. of Eng., Assoc. Prof. of Civil Eng., Tokyo Institute of Technology (Ookayama, Meguro-ku, Tokyo)

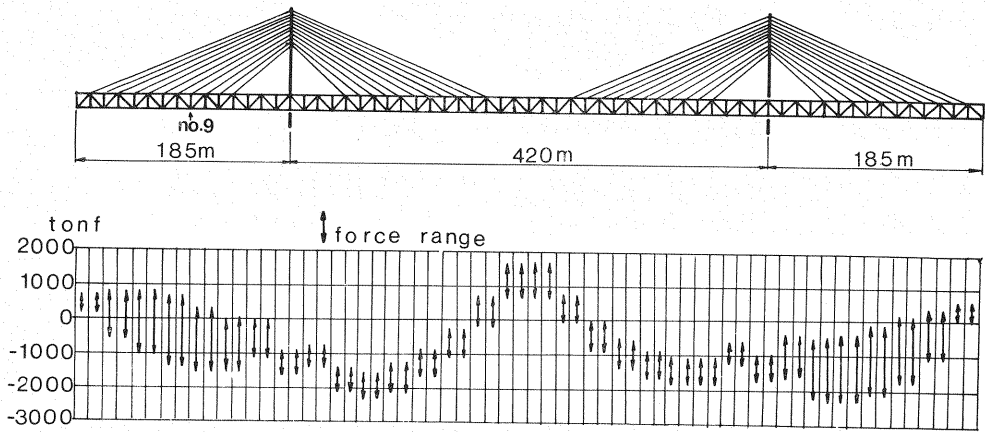


Fig.1 Force-ranges in lower chords of Hitsuishijima Bridge and Iwakurojima Bridge.

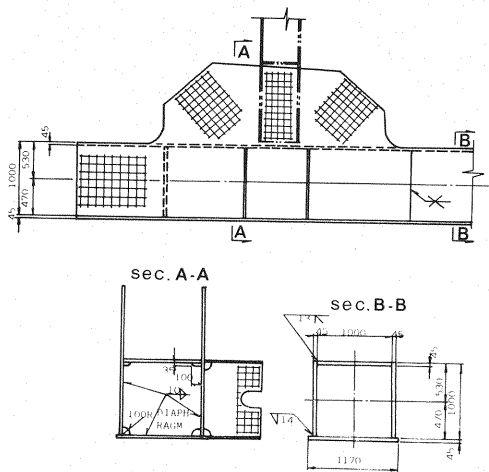


Fig.2 Details of lower chord at panel-point No. 9.

2. TEST SPECIMENS

The configuration and dimensions of a specimen are shown in Fig. 3. A pair of ribs, 25 mm thick, is attached to a main plate, 45 mm thick, 300 mm wide and 2400 mm long. The main plate and the ribs are made of SM 58 and SM 41 steels respectively. The mechanical properties and chemical compositions of these steels are shown in Table 1.

Longitudinal bead welding was performed in order to create residual stress at the location corresponding to the ends of the scallops. The longitudinal-bead welds were made by providing two lines of grooves on each side of the main plate by gouging. After the gouging, submerged arc welding was performed. The reinforcement of submerged arc welding was ground and the surface of the welds made smooth. The main plate was placed in a wooden member whose cross-section was 1 m×1 m, and the welding of the ribs onto the main plate was performed inside the wooden

study has the objective of obtaining basic data for the re-evaluation of the allowable design fatigue stress, in which the members are mostly subjected to repetitive compressive stresses.

In box-section truss members (Fig.2) , the fatigue strength of transverse fillet welds for attaching diaphragms in a box section is a decisive factor in the determination of the cross-section area. The fatigue strength of the joint is influenced by the profile of the toe of the fillet weld at the end of each scallop and the residual tensile stress introduced by corner welding. In order to study the effects of these factors, we fabricated actual size models of cruciform fillet welded joints. These joints include scallops and longitudinal weld beads. The design allowable stress for the Honshu-Shikoku bridges is revised based on these fatigue test results<sup>12)</sup>.

Table 1 Mechanical properties and chemical compositions of tested steels.

	THICKNESS (mm)	$\sigma_y$ (MPa)	$\sigma_s$ (MPa)	ELON- GATION (%)	IMPACT TEST (N-m)	C	Si	Mn	P	S	Cu	Ni	Cr	Mo	Nb	V	B	Ceq*	REMARKS
						x100			x1000			x100			x1000				
SM58Q	45	520	640	26	253(-5°C)	13	32	131	16	3	9	15		10		38	12	40	MAIN PLATE
SM41B	25	270	430	33	229( 0°C)	14	21	87	18	6									RIB PLATE

\*Ceq=C+Mn/6+Si/24+Cr/5+V/14+Ni/40+Mo/4

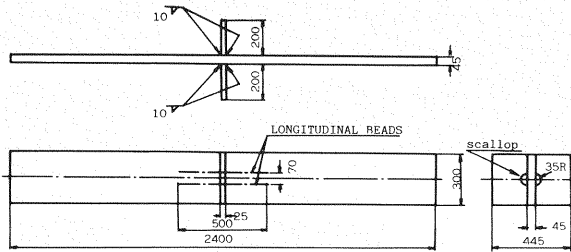


Fig. 3 Configurations and dimensions of specimen.

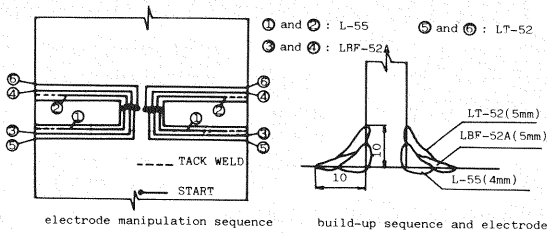


Fig. 4 Manipulation and build up sequence.

box, simulating the actual welding conditions. The sequences of electrode manipulation and building up of the weld metal are shown in Fig. 4. The electrode, "LBF 52", produced a smooth toe. All the weldings were started inside the scallops (see Fig. 4), and this procedure is the standard fabrication method used in the construction of the Honshu-Shikoku bridges.

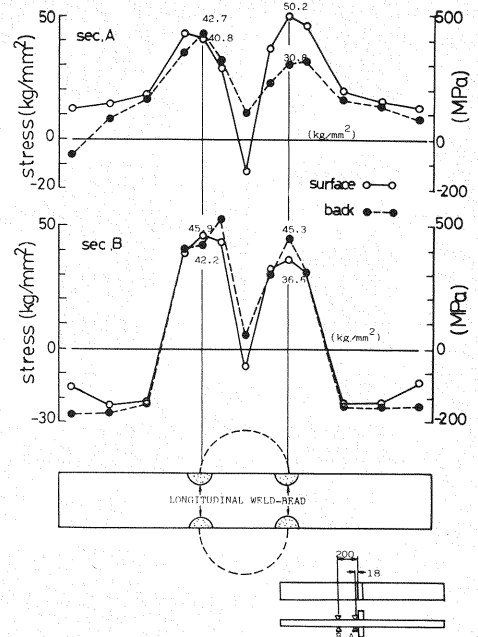


Fig. 5 Distributions of welding residual stresses.

### 3. RESIDUAL WELDING STRESS

Residual welding stress in an "as-welded" specimen was measured using the relaxation method. The length of the longitudinal beads in this experiment was 800 mm and longer than that used in the fatigue tests. The results of the measurements are shown in Fig. 5. The measurements were made at sections A and B. Section A was taken at 18 mm from the rib plate and section B at 200 mm from the rib plate. The residual stress at section B was considered to be unaffected by the welding of the rib plate to the main plate. In section B, the maximum residual tensile stress of approximately 440 MPa was recorded at the longitudinal bead weld, and residual compressive stress of approximately 250 MPa was produced near both sides of the specimen.

In section A, residual stresses mostly consist of tensile stress in the entire area. As shown in Fig. 5 (top figure), the tensile stress in section A is not balanced with the compressive stresses. However, the tensile and compressive stresses, which make up the residual stresses, are in balance in Section B (middle figure, Fig. 5). The apparent imbalance in section A can be explained the following way: the residual stress in section A can consist of multiple welding efforts from the fillet welding of the rib plates and the longitudinal weld beads. Therefore, when the stresses are measured on the surface, the imbalance was recorded. However, if directional stresses inside the plate, in three directions, were considered, the residual stresses should have been in good balance.

#### 4. METHOD OF FATIGUE TESTING

Fatigue tests were performed with an electro hydraulic fatigue testing machine of 4 MN dynamic capacity. The rate of loading was 5 Hz and the loading waveform was sinusoidal. Since it has been found in past studies that there is almost no difference in the fatigue strengths between completely pulsating and completely alternating tensions in welded members<sup>3)</sup>, the purpose of this paper is to study the fatigue behavior under stress conditions where the proportion of compressive stresses is dominant. In the experiments, the ranges of stresses were set at 196 MPa and 147 MPa. The tests were performed with stress ratios ( $R$ ) at 0,  $-1$ ,  $-2$  and  $-5$ . Furthermore, to clarify the

initiation and growth of fatigue crack, beach marks were created by halving the stress range at every certain number of stress cycles.

5. RESULTS OF FATIGUE TESTS

(1) Fatigue Strength

A summary of test results is shown in Table 2. The relationship between stress ranges ( $Sr$ ) and failure life ( $N_f$ ) is shown in Fig. 6. The number of cycles during the half-stress range is not included in the  $N_f$ . Regarding specimen S-9, since failure did not occur even with initial conditions of  $Sr=147$  MPa and  $R=-5$ , retesting was performed at  $Sr=176.4$  MPa and  $R=-5$ . At these conditions, the specimen finally failed. Fatigue lives were in the order of  $R=-1, 0, -2, -5$  at  $Sr=147$  MPa, and  $R=0, -1, -2, -5$  at  $Sr=196$  MPa. However, the differences of the lives among different specimens were not so great. The maximum stress in these tests for  $R=-5$  was 32.3 MPa at  $Sr=196$  MPa, and 29.4 MPa at  $Sr=176.4$  MPa. Failures in these specimens occurred at very low maximum stress. The failure at such a low maximum stress was not predictable.

(2) Initiation and Growth of Fatigue Crack

Examples of fracture surfaces are shown in Photo 1, and the results of observations of beach marks are shown in Fig. 7. In eight specimens, excluding specimen S-9, fatigue cracks originated from the toe in the fillet welding at the end of the scallops. The location of crack initiation was found right before the point where welding starts running parallel to the longitudinal direction of the rib plate. This is the zone where high residual tensile stresses exist. Fig. 8 shows the result of measurements of the flank angle  $\theta$  and radius  $\rho$  at the toes of the welds. As can be observed from the figure, the welding at the corner is not as smooth as other sections, such as parallel regions to the longitudinal section of the rib. The observation of beach marks indicates that multiple minute cracks formed simultaneously and joined together to develop a semi-elliptical crack. In the above case, the growth behavior was not dependent on the stress ratios. In the case of S-9 specimen, the fatigue cracks started at the root of the fillet welds. The number of stress blocks (one block consisting of full and half-stress ranges) of the stress ranges, the number of beach marks and the size of the innermost beach mark produced first during the test are shown in Table 2. According to the results, it is clear that in specimens S-1, S-2, S-4 and S-7, the fatigue cracks originated

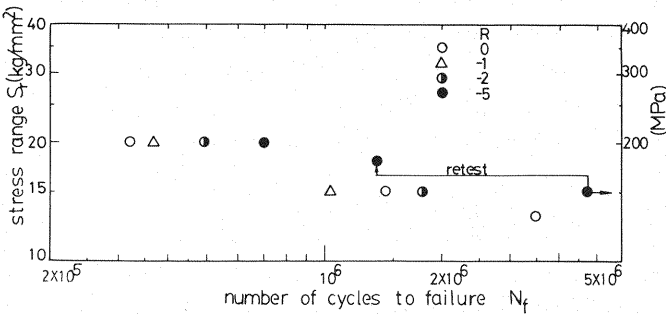


Fig.6  $Sr-N_f$  diagram.

at extremely early stages during the tests. Although the same tendency has not been confirmed in specimens S-6 and S-8 in the experiments, considering the fact that the beach marks were large in comparison to those of S-1, S-2, etc., we believe that similar phenomena have occurred in these specimens. However, a fatigue crack did not occur until  $4.7 \times 10^6$  cycles for  $Sr=147$  MPa in the S-9 specimen. As the stress

Table 2 Fatigue test results.

SPECIMEN	Smax	Smin	Sr	R	Nf	NUMBER OF STRESS BLOCKS	NUMBER OF BEACH MARKS	NUMBER OF CYCLES AT INNERMOST BEACH MARK	SIZE OF INNERMOST BEACH MARKS (mm)	
	(MPa)	(MPa)	(MPa)		$\times 10^3$				depth(a)	width(2b)
S-1	98	-98	196	-1	370	3	3	$100 \times 10^3$	0.8	4.9
S-2	65	-131	196	-2	495	4	4	$100 \times 10^3$	0.5	3.0
S-3	32	-164	196	-5	700	6	5	$200 \times 10^3$	0.45	1.0
S-4	196	0	196	0	321	2	2	$100 \times 10^3$	2.1	8.9
S-5	64	-64	127	-1	3480	11	6	$1800 \times 10^3$	1.0	3.5
S-6	74	-74	147	-1	1028	3	2	$600 \times 10^3$	4.2	10.9
S-7	49	-98	147	-2	1792	5	5	$300 \times 10^3$	0.38	1.3
S-8	148	1	147	0	1414	4	2	$600 \times 10^3$	2.8	8.3
S-9	25	-123	147	-5	>4700					
retest	29	-147	176	-5	1361					

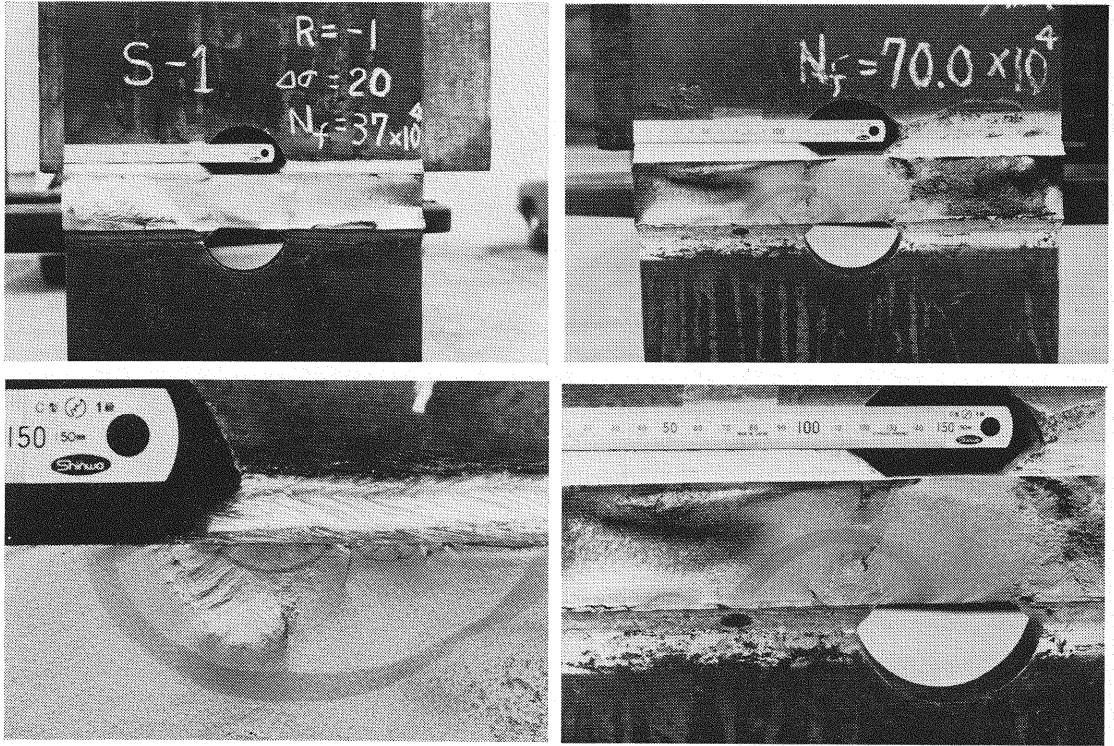


Photo 1 Fracture surfaces.

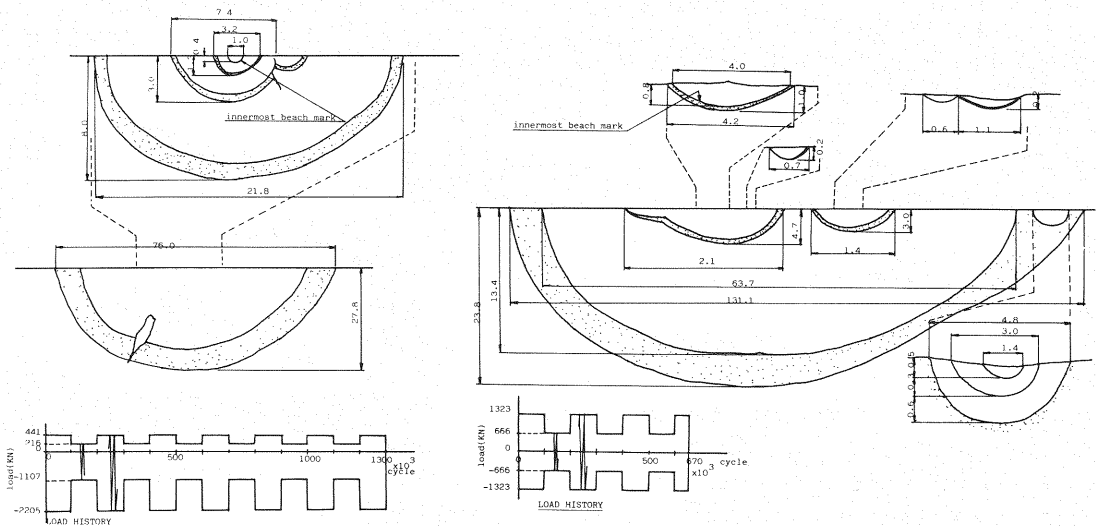


Fig. 7 Observation results of beach marks.

ratio and stress range became small, the ratio of the time required for the development of a crack and cause failure increased. The relationship between the fatigue crack growth rate ( $da/dN$ ) which is calculated from spacings between the beach marks and the stress intensity factor range ( $\Delta K$ ) for the crack is shown in Fig. 9. The crack was considered to be semi-elliptical, of depth " $a$ " and width " $2b$ ". The stress intensity factor range was calculated by the equation below by taking the influence of stress concentration due to the rib plate and fillet welds into account<sup>9)</sup>:

$$K = S r \sqrt{\pi a} F_g \times F_e \times F_s$$

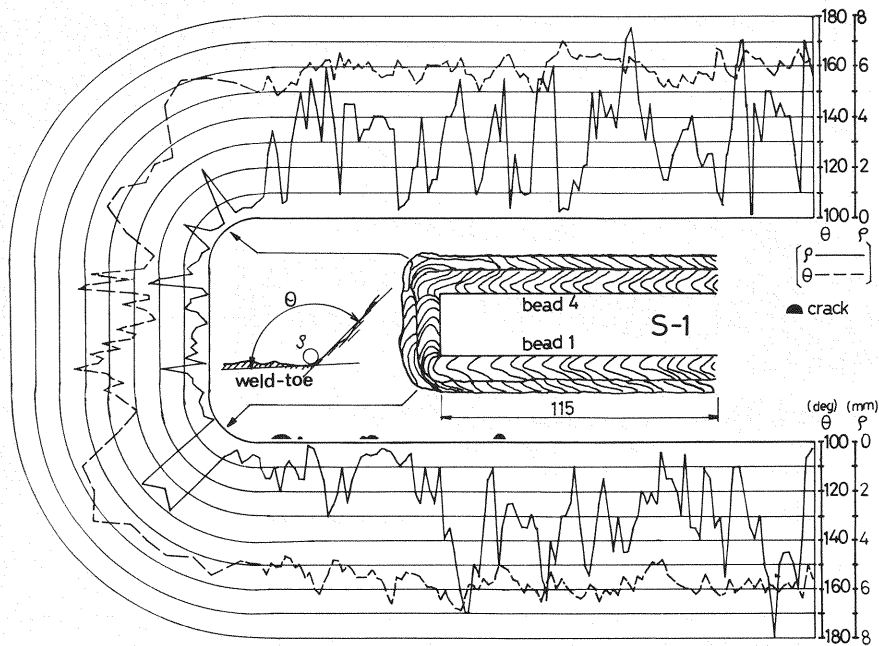


Fig. 8 Flank angle and radius at weld toe.

Where  $F_g$  is the correction factor for the stress gradient due to the joint configuration and fillet weld.  $F_e$  is the correction factor for the crack configuration, and  $F_s$  is the correction factor for the surface crack. The correction factors used here are as follows :

$$F_s = 1.12 - 0.12 \frac{a}{b}$$
$$F_e = \frac{1}{\int_0^{\pi/2} (1 - k^2 \sin^2 \varphi)^{1/2} d\varphi}, \quad k^2 = 1 - \frac{a^2}{b^2}$$

$F_g$  is computed using the finite element method. Fig. 10 shows the distribution of the computed stress and the  $F_g$  decay curve in the direction of the thickness of the plate at the weld toe. Data on the cracks which were found within 20–30 mm from the surface of the plate are plotted in Fig. 9 (indicated in Table 2).

In Fig. 9 a group of curves obtained by Ohta *et al.*<sup>(10)</sup> for SM 58 steel showing the relationship between  $da/dN$  and  $\Delta K$  for various values of  $R$ , are drawn in the same figure. As can be observed, most of the plot from the experimental data is located above the curve for  $R=0$ . This indicates that in the welded specimen used in the experiment, the crack growth rate is independent on stress ratio  $R$ . This means the crack growth life is independent on stress ratio  $R$ , which suggests that the expansion of fatigue life with the reduction of  $R$  is caused by the increase in the number of stress cycles required to initiate fatigue cracks.

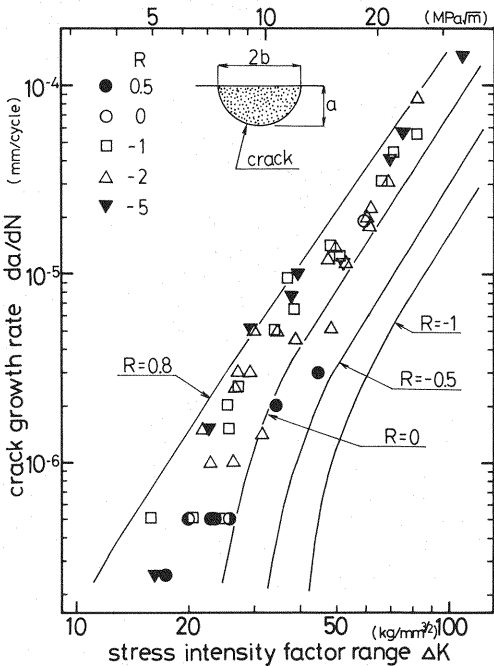


Fig. 9 Fatigue crack growth rate.

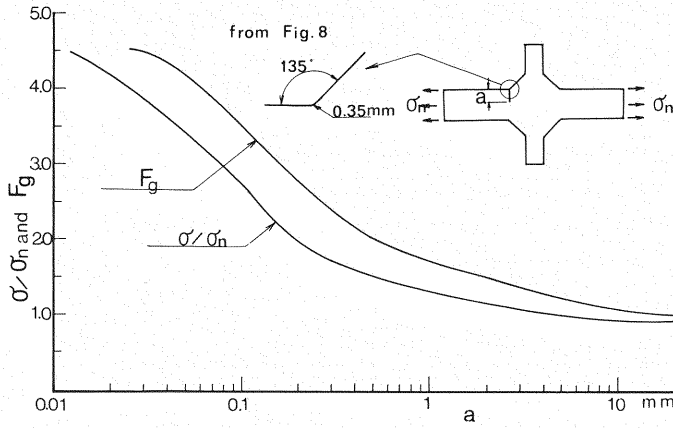
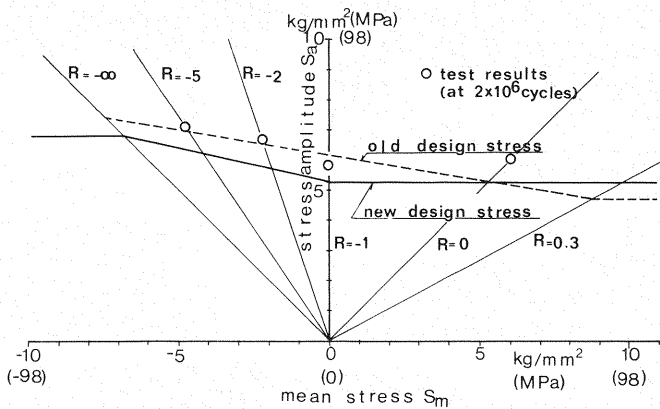
Fig. 10 Stress distribution and  $F_g$  decay curve.

Fig. 11 Test results and allowable stress range for category C.

## 6. DESIGN ALLOWABLE STRESS

Slopes of  $Sr-Nf$  relationships in the fatigue tests of various types of large welded joints produced for the Honshu-Shikoku Bridge Authority were approximately  $-1/3^{(1)}$ . Therefore, in order to estimate the fatigue strengths at  $2 \times 10^6$  cycles for various values of  $R_s$ , we assumed the slope of the  $Sr-Nf$  relationships to be  $-1/3$ . The estimated strengths at  $2 \times 10^6$  cycles were plotted in Fig. 11 with the abscissa representing mean stress ( $S_m$ ) and the ordinate stress amplitude ( $S_a = 1/2 S_r$ ). The transverse fillet welds belonging to the category C of the fatigue design code<sup>(1), (2), (12), (13)</sup> were constructed using a particular electrode. When this electrode is used, the profile of the weld toe can be made smooth. The allowable stresses for weld joints in Category C in the old design code are shown in Fig. 11. In the region where  $R$  is smaller than  $-1$ , there is no margin for safety. Particularly at  $R = -1$ , the test results (estimated fatigue strength) are below the allowable stress

defined by the old code. Therefore, the old code provides allowable stress values with little safety margin for negative values of  $R$ .

The allowable stress range for category C in the new design code is also shown in Fig. 11. The allowable stress for  $R=0$  is set to be the same as the value defined by the old code. To define the new fatigue allowable stresses for other values of  $R_s$ , a line which provides a constant safety margin to the test results was drawn (solid line, current design stress). As shown in Fig. 11 for positive values of mean stress, the line is parallel to the abscissa. For the allowable stress of  $R = -\infty$  (0—compression condition), the allowable stress intercepted the  $R = -\infty$  line at the point 30% higher than the allowable stress value which is estimated for the positive mean stress region. In the region of negative values of  $R$ , this new allowable stress is well below that defined by the old code.

## 7. CONCLUDING REMARKS

The principal findings obtained by the present study are as follows :

- i) The fatigue life of a cruciform welded joint with scallops and longitudinal weld-beads becomes longer as the value of  $R$  decreases. However, the difference in the lives is not very great.
- ii) In eight out of nine specimens, fatigue cracks initiated at the corner of scallops where the pattern of the weld toes was disturbed. Multiple fatigue cracks were produced adjacent to each other and these merged to develop into semi-elliptical cracks.
- iii) when the depth of the cracks was up to about one-half of the plate thickness, the fatigue crack growth rates did not differ for specimens of different stress ratios. As described in i), the failure life extends as  $R$  decreases.

This is considered to be mainly due to the difference in the properties of the initiation of the fatigue cracks and propagation when fatigue cracks are extremely small.

iv) Based on the test results of the study, the allowable fatigue stress range for Honshu-Shikoku bridges was revised. The allowable stress for  $R=0$  (minimum stress/maximum stress=0) is set to be equal to the value defined by the old code. Furthermore, we decided that this value is constant for all positive values of mean stress. For the value of  $R=-\infty$  (0—compression state), we determined that the allowable stress is 30% higher than that determined for positive values of mean stress. The allowable stress values between these two points ( $R=-1$  and  $R=-\infty$ ) are linearly interpolated between the above-mentioned values ( $S_r=125.4$  MPa and 163.0 MPa).

## ACKNOWLEDGEMENTS

The authors would like to thank all members of the Study Group on Fatigue, Sub-Committee of Steel Superstructures for Honshu-Shikoku Bridges in the Japan Society of Civil Engineers for their valuable suggestions.

The experimental work was carried out by Messrs. Y. Eguchi and S. Tanifuji of the Japan Construction Methods and Machinery Research Institute. The manuscript was prepared by Mr. T. Mori, Research Associate, of the Tokyo Institute of Technology.

The authors wish to express their sincere gratitude to all those mentioned above.

## REFERENCES

- 1) JSCE : The Specifications for Steel Railway Bridges, 1974 (in Japanese).
- 2) JSCE : Fatigue Design for Honshu-Shikoku Bridges, 1974 (in Japanese).
- 3) Hirt, M. A., Yen, B. T. and Fisher, J. W. : Fatigue Strength of Rolled and welded Steel Beams, Journal of the Structural Division, Proc. of ASCE, ST 7, pp. 1867~1911, 1971. 7.
- 4) Olivier, R. and Ritter, W. : Catalogue of  $S-N$  Curves of Welded Joints in Structural Steels, Uniform Statistical Analysis of Fatigue Test Results, DVS Report, No. 56, 1979.
- 5) AASHTO : Standard Specifications for Highway Bridges, 1977.
- 6) BS 5400, Part 10 : Steel, Concrete and Composite Bridges, Code of Practice for Fatigue.
- 7) Takahashi, C. and Kawai, Y. : Fatigue Strengths of Longitudinal Welded Joints under Compressive Stresses, Private letter.
- 8) Office for Research and Experiments of the International Union of Railways : D 130, Fatigue Phenomena in Welded Connections of Bridges and Cranes, April 1974.
- 9) Zettlemoyer, N. and Fisher, J. W. : Stress Gradient and Crack Shape Effects on Stress Intensity at Welded Details, Welding Journal, August 1978, 2465~2505.
- 10) Ohta, A., Sasaki, E. and Kosuga, K. : Effect of Stress Ratios on the Fatigue Crack Propagation Rate, Trans. of JSME, Vol. 43, No. 373, pp. 3173~3197, 1977 (in Japanese).
- 11) JSCE : Report on the Steel Superstructure of Honshu-Shikoku Bridges, Fatigue, 1981 (in Japanese).
- 12) JSCE : Report on the Steel Superstructure of Honshu-Shikoku Bridges, 1982 (in Japanese).
- 13) JSCE : The Specifications for Steel Railway Bridges, May 1983 (in Japanese).

(Received October 15, 1983)